Journal of Geodesy (2024) 98:86
https://doi.org/10.1007/s00190-024-01891-w

ORIGINAL ARTICLE

A robust approach to terrestrial relative gravity measurements and adjustment of gravity networks

Franco S. Sobrero[1] · Kevin Ahlgren[1,2] · Michael G. Bevis[1,6] · Demián D. Gómez[1] · Jacob Heck[1,3] · Arturo Echalar[4] · Dana J. Caccamise II[1,5] · Eric Kendrick[1] · Paola Montenegro[6] · Ariele Batistti[6] · Lizeth Contreras Choque[6] · Juan Carlos Catari[7] · Roger Tinta Sallico[6,7] · Hernan Guerra Trigo[7]

Received: 6 May 2024 / Accepted: 13 August 2024

Abstract
Like many geophysical observations, relative gravity (RG) measurements are affected by random errors, systematic errors, and occasional blunders. When RG measurements are used to build large gravity networks in remote areas under adverse environmental or logistical conditions (such as extreme temperatures, heavy precipitation, rugged terrain, difficult or dangerous roads, and high altitudes), it is more likely for significant errors to occur and accumulate. Therefore, obtaining accurate gravity estimates at regional gravity networks largely depends on defensive data collection protocols and robust adjustment techniques. In this work, we present a measurement field protocol based on highly redundant observation patterns, and a two-step least squares adjustment scheme implemented as a MATLAB package. This software helps us identify blunders, mitigates the impact of random errors, and downweights or removes outlier observations. The methodology also guarantees that adjusted gravity values have well-constrained standard error estimates. We illustrate the capabilities of our approach through the case study of the Bolivian gravity network, where we determined the acceleration due to gravity at 2548 stations that spread over difficult and sometimes extreme environments, with a typical level of uncertainty of 0.10–0.15 mGal.

Keywords Terrestrial relative gravimetry · Gravity network adjustment · Gravity survey field protocol

1 Introduction

Gravity surveys are conducted to measure and map the regional gravity field, serving multiple purposes. These include resource exploration, engineering projects, scientific research, tectonic studies, geoid determination, and the establishment of geodetic reference frames. The International Association of Geodesy emphasizes the need for all countries to carry out the necessary gravimetric surveys for the realization of the International Height Reference System (IHRS) (Poutanen and Rózsa 2020), especially densifying surface gravity networks in remote areas, to fill gravity data gaps (Sánchez et al. 2021).

These gravity networks are primarily constructed by measuring gravity differences using relative gravimeters that efficiently collect large amounts of surface gravity data rapidly and relatively inexpensively. The most common relative gravimeters nowadays are spring-based (Van Camp et al. 2017), where the gravity variations are measured by the changes in the length of a spring using different pick-off systems (optical, mechanical, or electrical amplification method to record spring extension) and transfer systems (Niebauer 2015). Relative gravity (RG) meters can operate in a wide range of environmental conditions and altitudes with an expected precision ranging from ± 0.01 to ± 0.10 mGal (Torge 1989; Rymer 1989) and with a reading

✉ Franco S. Sobrero
sobrero.1@osu.edu

1 Division of Geodetic Science, School of Earth Sciences, Ohio State University, Columbus, OH, USA

2 National Geodetic Survey, National Oceanic and Atmospheric Administration, Silver Spring, MD, USA

3 National Geodetic Survey, National Oceanic and Atmospheric Administration, Ann Arbor, MI, USA

4 Escuela Militar de Ingeniería, La Paz, Bolivia

5 National Geodetic Survey, National Oceanic and Atmospheric Administration, La Jolla, CA, USA

6 Central Andes Project, La Paz, Bolivia

7 Instituto Geográfico Militar, La Paz, Bolivia

Published online: 23 September 2024

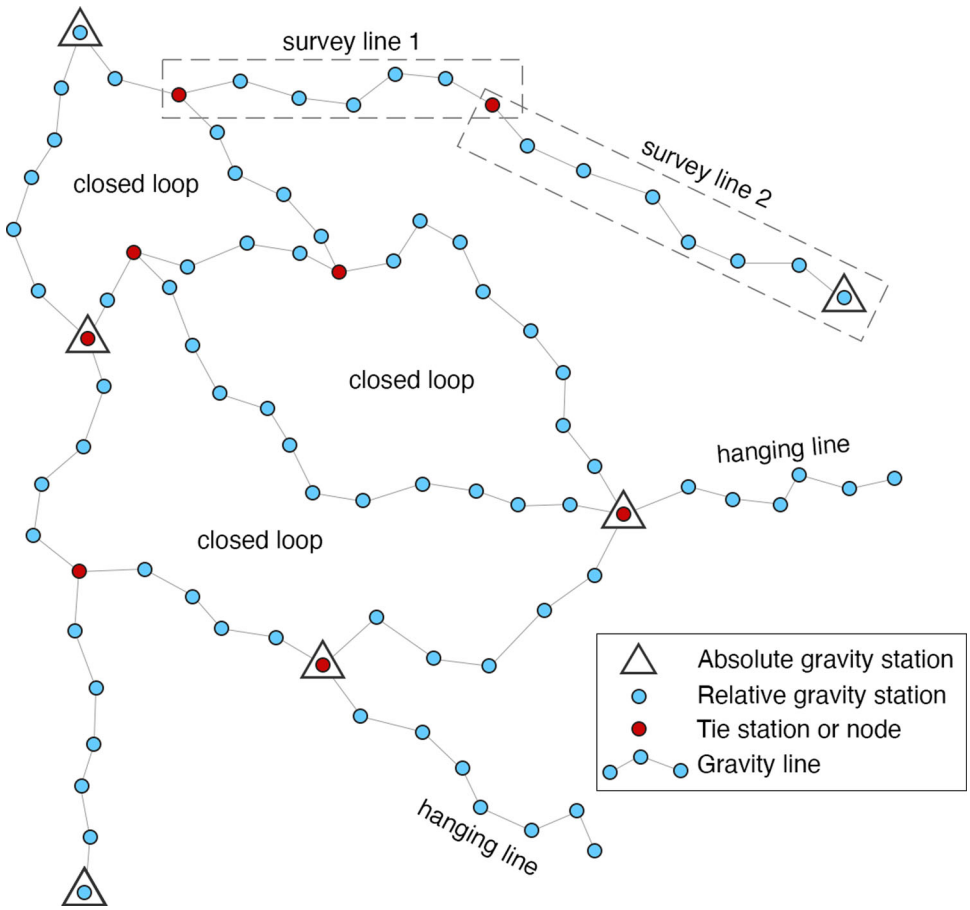

Fig. 1 Elements of a gravity network. Boxes in dashed line show consecutive survey lines connected by a tie station. For a complete description of the elements of a network, see the Glossary in the Supplementary Information

resolution as high as 1 μGal for some digital instruments (Scintrex Limited 2012).

As any other observation technique, gravity measurements are affected by blunders, systematic effects, and random errors. Blunders typically result from station misidentification, operator reading and recording errors, unstable voltage supply from the heating battery, and leveling errors (Kangieser 1983). They can often be detected through statistical analysis methods such as those described in Baarda (1967) and Koch (2013). Systematic effects are caused by groundwater changes, atmospheric effects, unmodeled calibration errors, instrument tilt, and most importantly, instrumental drift and gravity tides (Torge 1989; Bonvalot et al. 1998; Dias and Escobar 2001). The gravity tides affecting a stationary gravimeter can be accurately predicted and removed from gravimeter measurements using a gravity tide model (e.g., Büllesfeld 1985, Cartwright and Edden 1973, Cartwright and Tayler 1971, Doodson 1921, Longman 1959, and Tamura 1987), and these models normally include a correction that accounts for the solid Earth tide. Conversely, the drift rate is a parameter that needs to be estimated through the reoccupation of one or more stations in the gravity line, as it is mainly influenced by the ambient temperature (Fores et al. 2017), fluctuations in the instrument's internal temperature (LaCoste and Romberg 2004), transportation-related vibrations and shocks (Hamilton and Brulé 1967), and possibly by major changes in atmospheric pressure. Finally, random errors (which primarily result from environmental and transportation conditions, microseismicity, and the accumulation of random-walk-type effects) can be minimized through some form of adjustment. The most basic type of adjustment is often performed at a gravity line level, although a more robust approach involves the combination of gravity lines connected through tie stations, and occasionally tied to absolute gravity stations, to form a comprehensive surface gravity network (Fig. 1). The rationale behind this technique parallels the adjustment of spirit leveling networks, where incorporating closed loops and redundant observations improves the accuracy of the calculated heights.

The precision of the gravity values obtained through a network adjustment also depends on the quality of the input data. Well-defined data acquisition procedures or protocols are critical to minimize the noise level in the gravity measurements, especially when surveying gravity networks with hundreds or even thousands of stations spread out over large distances.

In this work, we present a methodology to survey, process, and adjust gravimetric networks of regional/continental

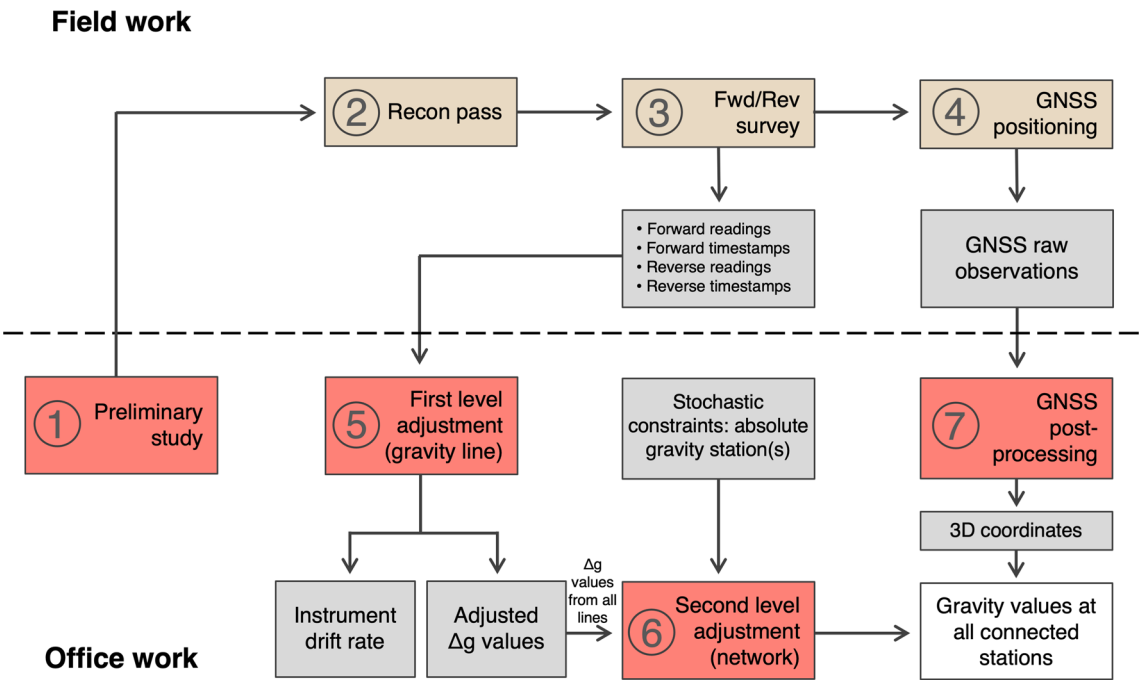

Fig. 2 Overview of the OSU field protocol and adjustment methodology. Numbers designate the activities' order. Beige boxes indicate field activities, red boxes indicate data analysis or processing tasks, gray boxes show either raw data or intermediate results, and the white box shows the final results of the network adjustment. For a detailed diagram of the first-level adjustment (Box 5), see Fig. 5

scale. This methodology consists of (a) a field protocol developed by the Geodesy and Geodynamics group in the Division of Geodetic Science at Ohio State University (hereafter, the OSU field protocol) more than 12 years ago, to collect RG data using massively redundant observation patterns and travel time measurements between station pairs, and (b) a two-step least squares adjustment, implemented as a MATLAB package (see Code Availability). Our methodology employs multiple gravimeters and occupies each station of the gravity line in both forward and reverse directions, following a 'ladder sequence' (FGCC 1984). While it is quite common to use this occupation pattern for a limited number of first-order gravity lines, we have adopted this protocol for surveying all gravity lines in the network, thereby ensuring an unusual level of redundancy in the observations. The advantages of this approach are threefold: (1) it enables unusually well-constrained gravity estimates, (2) it allows for the detection of outlier observations or blunders, and (3) it yields gravity uncertainties that are calculated based on large numbers of physically meaningful residuals.

Because we have always used the same RG measurement procedure in South America, and appear to have been the only geodesy or geophysics group to use it to build any large network in this continent, we refer to it as the OSU field protocol or the OSU measurement protocol. Our two-stage adjustment is designed to take maximum advantage of this protocol, and, as a result, it is best suited to adjusting gravity lines and networks collected using this protocol.

Previous studies have applied fairly similar methodologies to adjust RG networks, such as the weighted constraint model by Hwang et al. (2002). However, our approach combines an initial adjustment at the gravity line level, where the instruments' linear drifts are estimated and removed as recommended by Dias and Escobar (2001), and a second adjustment at a network level that minimizes closure errors and introduces the gravity datum through stochastic constraints.

We validate the performance of the OSU field protocol and the adjustment model by presenting the case of the Bolivian gravity network. The acceleration due to gravity was determined at 2548 stations distributed over a wide range of altitudes and environmental settings, with a typical level of uncertainty (1 sigma) of 0.10 to 0.15 mGal. To the best of our knowledge, this is the first nationwide surface gravity network in South America measured entirely using 'ladder' surveys with multiple gravimeters.

2 The OSU field protocol

The OSU field protocol has been designed to induce massive levels of redundancy to the measurements enabling us

to identify, localize and remove blunders, and mitigate the effects of random errors. It comprises four stages: preliminary study, reconnaissance pass, forward-reverse gravity survey, and the GNSS positioning survey (Fig. 2).

2.1 Preliminary study

A preliminary study is conducted before any field activity and consists of gathering data to anticipate potential setbacks during the campaign, such as roadblocks, severe weather, safety and health hazards, and logistical difficulties. Possible sources of information to consult at this stage include reports from public agencies regarding existing geodetic networks (bench marks, coordinates, monument specifications and state of preservation, markers metadata, etc.), topographical maps, road maps, satellite images, weather forecasts, governmental travel advisory reports, and local news reports on protests, blockades, landslides, etc., in the area. As the gravity network grows farther from main roads and toward remote locations, the preliminary study (as well as the reconnaissance pass) becomes increasingly relevant for the success of a survey. Compared to other types of geodetic and topographical campaigns, gravity surveys add two critical considerations to the campaign planning phase: the limitations imposed by the maximum allowable closure time for the projected gravity lines (see Sects. 2.3 and 3) and the transportation conditions that affect the instrument drift (Hamilton and Brulé 1967; LaCoste and Romberg 2004). Thus, when projecting the geometry of a gravity network, it is essential to consider the accessibility of the sites, the travel time between them, and the condition of the roads and their surroundings.

2.2 Reconnaissance

The initial reconnaissance survey, or 'recon pass' or 'recce,' should be conducted at least a few weeks before the gravity survey. This allows enough time to evaluate the gathered information and adjust the campaign plan accordingly. The primary objectives of the reconnaissance are:

(a) Scouting local roads to assess their overall conditions and identify roadblocks or closures in situ.
(b) Locating survey markers, evaluating their condition, and repairing or replacing them if needed, or, where there are no markers, selecting the sites and installing survey markers.
(c) Anticipating realistic travel times between stations.
(d) Assessing the sky view at the sites for optimum GNSS positioning, clearing vegetation, or, if necessary, finding alternative locations nearby.

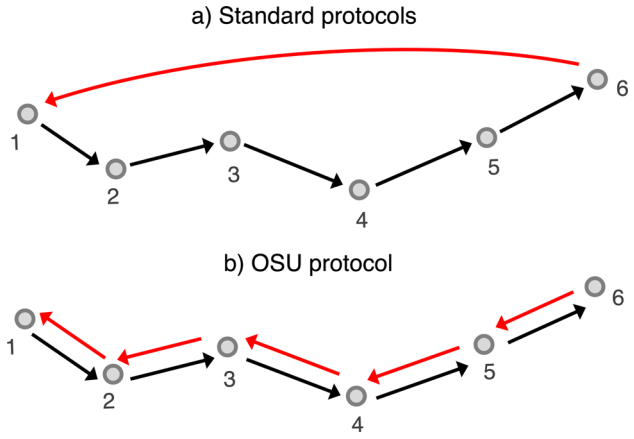

Fig. 3 Relative gravity observation pattern of a gravity line with six stations implementing **a** the standard occupation protocol used in South America, and **b** OSU's field protocol. Numbers 1–6 identify the gravity stations, and the black and red arrows indicate forward and reverse survey directions, respectively. The OSU field protocol involves stopping at least a few minutes (or an overnight stop in some cases) before the reverse measurements start. Thus, the last station (#6) is observed twice, just like all the others

2.3 The spatial pattern of 'forward-reverse' surveys of individual gravity lines

OSU's measurement protocol is designed to achieve very high degrees of redundancy, and our two-stage adjustment process is focused on fully exploiting that redundancy. In this section, we describe our measurement protocol and its advantages, and we introduce the first-stage adjustment that is performed one gravity survey line at a time. (The second stage adjustment applies to the network as a whole, and it ingests the results from the first-stage adjustments for every line in the network, plus all information for collocated absolute gravity stations.)

We define a gravity line as a local set of gravity stations that are occupied using one or more relative gravimeters within 24 h (in some extreme settings within 36 h), in such a way that we can estimate the drift rate, $\dot{D}$, of the gravimeter by assuming that $\dot{D}$ is constant throughout the survey of the line. We must estimate the value of this drift rate parameter (for each gravimeter used in the survey) in order to remove spurious temporal changes in the measured value of gravity.

The most common and conventional approach to measuring a gravity line is to visit each gravity station in turn and then double back to reobserve one of those stations (typically the first station) so as to enable an estimate of the gravimeter's drift rate, since, once the measurements have been corrected for gravity tides, the apparent change in gravity is mostly that due to instrument drift. The most common approach is shown in Fig. 3a. There are two obvious frameworks for discussing measurements and the degree of redundancy for

any spatial pattern of measurement: one focused on (biased) gravity values and the other on gravity differences. These frameworks are mathematically equivalent, although, in our opinion, the simpler framework conceives the two successive measurements of gravity m_k and m_{k+1} made using a *relative* gravimeter as a single observation of the difference $\Delta m = m_{k+1} - m_k$. The quasi-observation Δm is related to the actual difference in gravity, $\Delta g = \Delta m + \dot{D}\Delta t$, where Δt is the time taken to travel from station k to station $k + 1$ (see Sect. 6.1). If we record the times of each station occupation, we can estimate $\dot{D}$ from the data collected during the course of the survey, and so get what we need—the Δg values—from what we observed—the Δm values. Suppose that the total time that passes between the first and second occupation of station 1 (Fig. 3a) is T. Then, we can estimate the drift rate using the equation $\dot{D} = ({m_1}^F - {m_1}^S)/T$ where ${m_1}^F$ is the first measurement at station 1 at the beginning of the survey and ${m_1}^S$ is the second measurement at the end of the survey. The parameters we wish to infer from the conventional survey (Fig. 3a) are the five independent values of Δg plus the nuisance parameter $\dot{D}$, a total of six unknowns. Because we doubled back to reobserve station 1, there are a total of six known Δm values. So, there are six knowns and six unknowns, the estimation problem is evenly determined, and there is no measurement redundancy at all.

Under OSU's measurement protocol (Fig. 3b), every station along the gravity line is visited twice—once during the forward leg and once during the reverse leg of the survey. Unlike the standard occupation procedure (Fig. 3a), where only one station is revisited to produce an evenly determined solution, our standard procedure (Fig. 3b) produces observational redundancy and an overdetermined least squares problem for the gravity line analysis or first-stage adjustment. For a one-gravimeter survey, we need to estimate the five Δg values and $\dot{D}$, but now we have 10 Δm observations, and therefore an overdetermined least squares problem with four degrees of freedom in the residuals. That is, there are four degrees of redundancy. If we ran this survey (Fig. 3b) using two gravimeters, we would have to estimate one more parameter (the drift rate for the second gravimeter), but we would now have 20 Δm observations, and so 13 degrees of freedom in the residuals. Combining the backward-forward occupation geometry of Fig. 3b with the use of two or more gravimeters produces *massively* redundant observational datasets (see Table 1).

Moreover, the diagnostic power of standard protocols (Fig. 3a) is limited, as it is very difficult if a major error has occurred, or when a network analysis suggests that it has, to determine *where* along the line this major error has occurred, even when employing more than one gravimeter. The observation pattern of the OSU field protocol, in contrast, allows for a thorough analysis of every station pair and each gravity meter individually, and guarantees redundant observations even with a single instrument. Furthermore, since all readings are used in the drift estimation (see Sect. 6.1), a reading error at one reoccupied station need not undermine the adjustment of the entire gravity line, as it would with a standard observation pattern. If we use our residuals to determine that gravimeter B made a bad measurement at station 3, for example, we can drop that station from the analysis of the line being measured with gravimeter B, but not from the survey line being measured with gravimeter A.

Due to multiple factors that are further discussed in Sect. 3, the entire forward-reverse occupation of a line should conclude within 36 h. The gravity survey typically starts around dawn and should conclude before nightfall, as performing gravity observations in the dark often results in operator errors. Lines are driven with stops of 30–50 min to measure gravity at the designated stations. In areas with many poor and very slow roads, like Bolivia (Sect. 7), the forward line may be measured throughout one day, with the reverse portion of the survey taking place the following day. Thus, a survey line composed of stations A to E, for instance, presents the following occupation pattern: day 1 (forward) A-B-C-D-E and rest overnight, day 2 (reverse) E-D-C-B-A. Alternatively, the entire forward-reverse survey may be carried out on the same day, and there should be a short break between the first and second observation of E. In single-day line surveys, the forward measurements must conclude in the early afternoon, allowing enough time to finish the reverse observations before dusk. In terms of spatial resolution, we typically choose station locations so that the distance between two consecutive stations is between 12 and 18 km, and does not exceed 20 km. This separation allows the survey to cover large areas quickly, while it guarantees that consecutive stations are affected by almost the same atmospheric effects (Goodkind 1986; Merriam 1992).

2.4 GNSS positioning survey

It is necessary to determine the geodetic coordinates of the gravity stations to compute the gravimetric anomalies. Precise positioning is achieved through static GNSS measurements, with a target precision set by the vertical gravity gradient and the instrumental precision. The normal vertical gradient (using the values of the Geodetic Reference System 1980) is 3086 ns^{-2} (Torge 1989), or 0.3086 mGal/m, while the mean expected measurement precision of a relative gravimeter operating in field conditions (large gravity differences, motor vehicle transport through rugged terrain, and station separations of > 10 km) is approximately ± 0.06 mGal. Therefore, the stations' vertical position is to be determined with an accuracy better than ± 0.20 m. This precision can be achieved with two-hour static GNSS occupations using free post-processed PPP services (Grinter and

Table 1 Comparison of the degrees of freedom (DoF) of a gravity line adjustment, when surveyed following the OSU field protocol and a standard protocol

			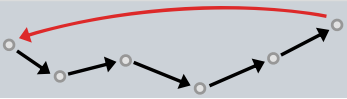	
Number of gravimeters used	1	Observations	6	10
		Unknowns	6	6
		DoF	**0**	**4**
	2	Observations	12	20
		Unknowns	7	7
		DoF	**5**	**13**
	3	Observations	18	30
		Unknowns	8	8
		DoF	**10**	**22**
	4	Observations	24	40
		Unknowns	9	9
		DoF	**15**	**31**

Example case of a line with six stations measured with 1–4 gravimeters. Note that the number of observations refers to the number of quasi-observations, Δm, as described in Sect. 2.3

Janssen 2012; Shouny and Miky 2019; Diouf et al. 2023) and online differential positioning services (Eckl et al. 2001; Soler et al. 2006). At sites with suboptimal sky views, three-hour occupations are recommended. Due to these extended occupation times, the GNSS survey should be carried out independently from the forward-reverse gravity survey.

3 Line closure time

There has yet to be a consensus over the maximum acceptable closure time for gravity lines to build a gravity network. Gravimetry field manuals recommend line closure times that range between 4 and 48 h (Murray and Tracey 2001; Hinze et al. 2013; IGN 2014; INEGI 2015; IBGE 2017). Such wide variability is mainly due to two reasons: (1) it is difficult to determine the maximum time interval at which a gravimeter drift rate becomes significantly nonlinear, and (2) the effects of incorrectly assuming drift rate linearity will vary depending on several factors such as the choice of gravimeter, the station occupation pattern, observation redundancy, and adjustment method. Figure 4a illustrates that reducing the total survey time makes the drift correction for LaCoste-Romberg G-meters less accurate. As the measurement time is reduced and fewer stations are occupied, separating purely random measurement error from instrumental drift becomes increasingly difficult. The OSU field protocol contemplates a maximum line closure time of 36 h. However, the logistical constraints are sometimes so severe that it becomes impractical (or even impossible) to return to a site within this time frame. Thus, longer closure times are permitted when working in extreme circumstances. The results from the Bolivian gravity network presented in Fig. 4b show that increasing the closure time does not significantly impact the magnitude of a line's residuals.

Finally, the project manager should also factor the logistical costs of the gravity campaign into the definition of the optimum line closure time. In some cases, the benefits of increasing the number of stations occupied per day might outweigh the negative impact that extending the closure time has on the residuals' scatter level (~ 0.9 μGal/h, from Fig. 4b). Ultimately, higher productivity can reduce overall costs, allowing the building of larger, high-accuracy gravity networks.

4 Data collection

The gravity survey crew employs a minimum of two gravimeters (ideally three or four) to take independent measurements

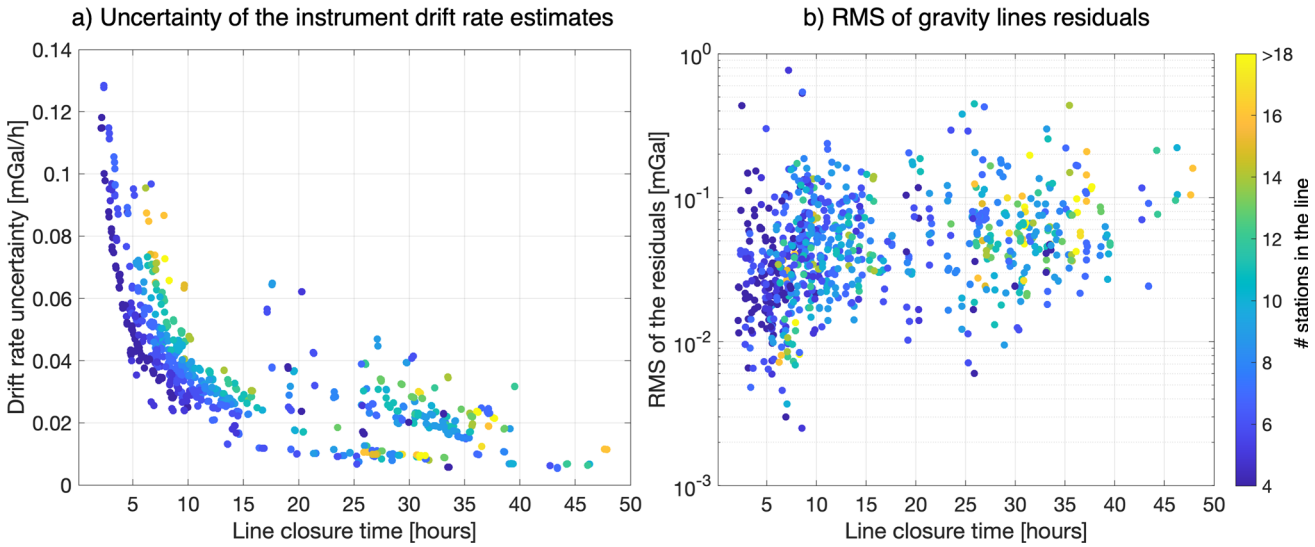

Fig. 4 Results from gravity line adjustments in the Bolivian gravity network. **a** Uncertainty in the instruments' drift rate estimates (per gravimeter, per gravity line) as a function of line closure duration. Uncertainties computed with $\sigma_0 = 0.01$ mGal. **b** RMS of the residuals of line adjustments as a function of line closure duration. Colors represent the number of stations in the gravity line. For clarity, results for lines longer than 50 h are not shown. Gravity lines with less than four stations are excluded, as the number of residuals is insufficient to compute a reliable RMS value

at each station in the forward and reverse directions. For optimum results, each and every RG meter should have a single designated operator throughout the entire campaign. This helps to identify the effects of potential systematic errors in the readings by means of comparison between gravimeters. Three independent measurements (per instrument) are taken within five minutes. At the beginning of every work day, each operator conducts a sensitivity test following user manual instructions (LaCoste and Romberg 2004) to ensure that the levels and sensitivity settings are appropriately adjusted.

During each occupation, the operators should follow these steps:

1. Assign a unique code to the station, maintaining a consistent character length for all stations within the network.
2. Perform three RG readings
3. Fill in all fields of the data log form: station code, date, UTC Time, latitude and longitude of the site, RG readings, instrument internal temperature, vertical offset (see Supplementary Information), and comments (weather conditions, traffic, vibration level, instrument internal temperature fluctuations, etc.)
4. Take a GNSS waypoint at the station with a hand-held receiver
5. Take a picture of the site
6. Take a picture of the instrument with the counter and the nulling dial visible. This can be used a posteriori to amend transcription errors.

We developed an Android application called Log4G (see Code Availability) to collect georeferenced and time-tagged RG data using mobile devices. This app was specifically designed to comply with the OSU field protocol. Among many features, it performs real-time data quality and line closure controls that reduce the occurrence of reading blunders and time recording errors.

Regardless of the data recording method (electronically or on paper), the operator should verify that the readings' transcriptions are correct and the instrument remains leveled after concluding the measurements. Having the utmost confidence in the measurements before leaving the survey area is crucial, especially when working in remote and hard-to-access locations.

5 Transportation

RG readings are strongly affected by shocks acting during transport and measurement. Large disturbing accelerations cause reactions in the measurement system, inducing reading jumps or 'tares' in the order of μms^{-2} (Torge 1989) and affect the rate of instrumental drift (Hamilton and Brulé 1967). In fact, Lambert et al. (1979) evaluated various transport methods, including hand, motorized vehicles over good and bad roads, and helicopters, and showed that the instrument drift is a function of the transportation type. Scintrex CG5 meters, in particular, present a high tilt susceptibility, which affects the readings after being tilted for moderate periods of time during transit (Reudink et al. 2014; Klees et al. 2019).

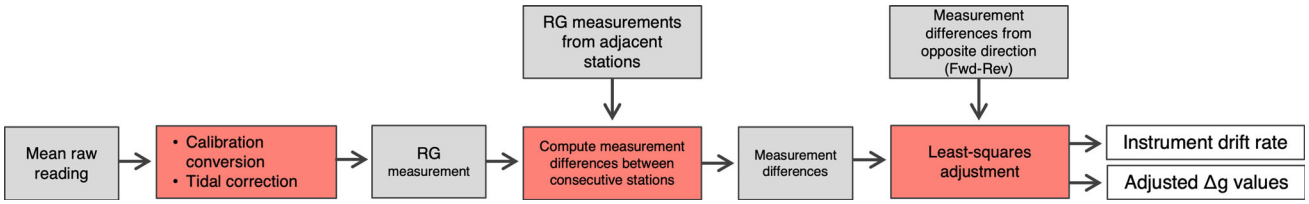

Fig. 5 First-level adjustment overview for a single gravity line with a single gravimeter. Red boxes denote data processing tasks, gray boxes indicate either raw data or intermediate results, and white boxes indicate the final results of the gravity line adjustment

It is possible to minimize the effects of transport-related effects by taking special precautions, such as choosing vehicles with softer suspension, driving more slowly on very poor roads, wrapping the meter carrying case with foam or similar shock-absorbing materials, hand-holding the instrument off the seat to reduce the vibration transmitted from the vehicle while keeping it as vertical as possible, etc. Neglecting the care of each gravimeter during transportation can jeopardize the success of the gravity survey. Alternative modes of transportation, such as horseback, boats or helicopters, may be considered for exceptionally inaccessible settings. We occasionally reached some very high mountain stations on foot.

6 Adjustment methodology

The adjustment methodology consists of two independent least squares fits performed sequentially. A first fit is conducted for each gravity line to estimate and remove the instrument drift and compute the gravity differences between the line stations. The second-level adjustment combines the adjusted gravity differences from all the connected gravity lines into a single network adjustment. It imposes absolute gravity (AG) constraints and loop closures (see Hanging line in the Supplementary Information) to produce well-constrained gravity estimates at every station of the network.

6.1 First-level adjustment: the gravity line

The gravity line adjustment is conducted individually for each gravimeter. It yields estimates of the gravity differences between adjacent stations (Δg values) and the instrumental drift rate estimate. The input data are the raw readings and the measurement times expressed in UTC (Fig. 2).

First, we assess the overall data quality by evaluating (1) the standard deviation of the three readings taken at each site to detect blunders, (2) the difference between the forward and reverse readings to identify transcription errors, and (3) the mean velocity between stations computed using their coordinates and the measurements timestamps, as unusually high or low velocities might indicate errors in measurement time recordings. Figure 5 presents a step-by-step description of the gravity line adjustment after data cleaning.

The mean raw reading (average value of the three readings) undergoes a calibration conversion that transforms 'counter units' to gravity units (required for some RG meters, such as the LaCoste & Romberg Model G) and a tidal correction. The calibration correction is derived from calibration curves the manufacturer provides for each instrument. To ensure the accuracy of these calibration factors, it is essential that the instruments are serviced regularly and are subjected to periodic calibration tests. Conversely, the gravity tide effect can be removed using physical models. We use the formulation developed by Longman (1959). While other models are more suitable for microgravity studies (Bonvalot et al. 1998), the precision of Longman (1959) is acceptable for large-scale gravity networks. Our gravity tide models and codes, used in data reduction, incorporate both the direct (astronomical) gravity tide and the cyclical variation in gravity due to gravimeters' rise and fall in response to the solid Earth tide.

The resulting reduced value (mean raw reading corrected for calibration and tidal effects) is the RG measurement. The observation equation for an RG measurement m at station Q is

$$m_Q = g_Q - M_0 + D(t_Q) + e_Q \tag{1}$$

where g_Q is the gravity value and M_0 is a level unknown (or constant bias). The measurement is affected by a time-dependent bias $D(t)$ due to the gravimeter drift and a random error e_Q, which is assumed to follow a normal distribution. The gravimeter drift D at a time t can be expressed as a first-degree polynomial:

$$D(t) = \dot{D} \cdot (t - t_0) \tag{2}$$

where t is the measurement time, t_0 is the reference time, and $\dot{D}$ is the linear drift rate.

The observed measurement difference Δm between consecutive stations Q and R using a single gravimeter in the forward direction is.

$$\Delta m_{QR} = m_Q - m_R \tag{3}$$

Combining Eqs. (1), (2), and (3), we have

$$\Delta m_{QR} = \Delta g_{QR} - \dot{D} \cdot \Delta t_{QR} \tag{4}$$

where Δg_{QR} is the gravity difference to be estimated, and Δt_{QR} is the time elapsed between the measurements at Q and R. The level unknowns from Eq. (1) are canceled. Since gravity measurements are independent, it is reasonable to consider no covariance between them. While some physical correlations might be present in the observations due to imperfect drift modeling and other systematic errors, the magnitude of such correlations is unknown beforehand and may only be estimated from post hoc empirical covariance analyses (Torge 1989).

The gravity difference between consecutive stations Q and R is such that $\Delta g_{QR} = -\Delta g_{RQ}$. Hence, the observation equation for the measurement in the reverse direction is

$$\Delta m_{RQ} = -\Delta g_{QR} - \dot{D} \cdot \Delta t_{RQ}. \tag{5}$$

For a complete gravity line composed of a set of stations $\mathbf{U} = \{U_1, U_2, U_3, \ldots, U_{n-1}, U_n\}$, the matrix form of Eqs. (4) and (5) is:

$$\begin{bmatrix} \Delta m_{U_1U_2} \\ \Delta m_{U_2U_1} \\ \Delta m_{U_2U_3} \\ \Delta m_{U_3U_2} \\ \vdots \\ \Delta m_{U_{n-1},U_n} \\ \Delta m_{U_n,U_{n-1}} \end{bmatrix} = \begin{bmatrix} 1 & 0 & \cdots & 0 & -\Delta t_{U_1U_2} \\ -1 & 0 & \cdots & 0 & -\Delta t_{U_2U_1} \\ 0 & 1 & \cdots & 0 & -\Delta t_{U_2U_3} \\ 0 & -1 & \cdots & 0 & -\Delta t_{U_3U_2} \\ \vdots & \vdots & \ddots & \vdots & \vdots \\ 0 & 0 & \cdots & 1 & -\Delta t_{U_{n-1},U_n} \\ 0 & 0 & \cdots & -1 & -\Delta t_{U_n,U_{n-1}} \end{bmatrix} \times \begin{bmatrix} \Delta g_{U_1U_2} \\ \Delta g_{U_2U_3} \\ \vdots \\ \Delta g_{U_{n-1},U_n} \\ \dot{D} \end{bmatrix}. \tag{6}$$

We solve the linear system of Eqs. (6) using least squares with uniform weights as

$$\mathbf{b} = (\mathbf{A}^{\mathrm{T}}\mathbf{A})^{-1}\mathbf{A}^{\mathrm{T}}\mathbf{y} \tag{7}$$

where $\mathbf{b}$ is the vector of unknowns (gravity estimates and instrument drift rate), $\mathbf{y}$ is the vector of measurement differences (quasi-observations), and $\mathbf{A}$ is the model matrix (also known as the design matrix).

The residuals of the line adjustment, computed as $\mathbf{r} = \mathbf{y} - \mathbf{Ab}$, serve as diagnostic tools to evaluate the quality of the adjustment, detect outlier observations, and provide insights into the nature of the errors present in the data. For instance, a gravimeter tare would be evident in a line residual plot. Considering a reference performance of $1\sigma = 0.1$ mGal, the value of the residuals within a line should not exceed $\pm$ 0.3 mGal ($\sim 3\sigma$).

Since each instrument produces an independent set of predicted Δg values in a line, it is possible to conduct a comparative analysis between devices. This analysis also allows for blunder detection and may reveal systematic errors related to an underperforming instrument (Fig. S1). If Δg estimates from different gravimeters differ by more than 1σ, then the raw readings should be scrutinized and fixed whenever possible. If the source of the discrepancy cannot be identified, the inconsistent observations should be excluded from the corresponding gravimeter's adjustment and, ideally, remeasured. The robust adjustment approach and comprehensive gravity line-level analyses generate consistent and redundant estimates of the Δg values, which are the primary input of the subsequent gravity network adjustment.

6.2 Second-level adjustment: the gravity network

A network adjustment combines Δg values from multiple gravity lines to produce AG estimates at all stations. A collection of connected RG lines, surveyed exclusively with relative gravimetry, can be adjusted as a free network (Van Mierlo 1980). However, this approach will not yield an AG solution due to its intrinsic datum deficiency: estimating AG values through a least squares adjustment by solely measuring gravity differences is impossible. The datum deficiency can be overcome by incorporating AG measurements into the least squares fit. We opt to introduce them as stochastic condition equations (SCEs) with weights proportional to the uncertainties of the AG measurements. In the same way as regular observations, SCEs produce minimized residuals during the adjustment.

Firstly, we form the normal equations for the RG observations

$$\mathbf{N} = \mathbf{B}^{\mathrm{T}}\mathbf{PB} \tag{8}$$

$$\mathbf{c} = \mathbf{B}^{\mathrm{T}}\mathbf{Pd} \tag{9}$$

where $\mathbf{B}$ is the design matrix, $\mathbf{d}$ contains the observed gravity differences (first-level adjustments outputs), and the weight matrix $\mathbf{P}$ is formed according to the scheme described in Sect. 6.3. Here, we use $\mathbf{B}$ to distinguish it from the design matrix of the line adjustment in Eq. (7). Each row in $\mathbf{B}$ corresponds to a drift-free Δg, and each column corresponds to an individual station. Therefore, Δg values obtained with multiple gravimeters are represented in $\mathbf{B}$ by repeated rows.

Analogously, we can form normal equations for the SCEs:

$$\mathbf{N}_{\mathrm{K}} = \mathbf{K}^{\mathrm{T}}\mathbf{P}_{\mathrm{K}}\mathbf{K} \tag{10}$$

$$\mathbf{c}_{\mathrm{K}} = \mathbf{K}^{\mathrm{T}}\mathbf{P}_{\mathrm{K}}\mathbf{d}_{\mathrm{K}} \tag{11}$$

where $\mathbf{K}$ is the matrix of coefficients (populated with ones at constrained stations and zeros at all others), $\mathbf{P}_{\mathrm{K}}$ contains the SCEs weights, and $\mathbf{d}_{\mathrm{K}}$ is the vector of AG measurements. Finally, the constrained least squares solution of the gravity network is given by:

$$\overline{\mathbf{x}} = (\mathbf{N} + \mathbf{N}_{\mathrm{K}})^{-1}(\mathbf{c} + \mathbf{c}_{\mathrm{K}}) \tag{12}$$

where $\overline{\mathbf{x}}$ is the vector of adjusted gravity estimates at each station.

6.3 Weighting scheme

During the collection of RG data, the gravimeters employed are exposed to the same environmental conditions, as they are typically located nearby and operate nearly simultaneously. However, the scatter level of the line adjustment residuals is not equal across all instruments (Fig. S1). One of the main reasons for these discrepancies is the distinct operational performance of every gravimeter, even under identical conditions. To address this variability, we implement a scheme that assigns weights to the Δg observations based on each instrument's historical performance. Thus, the a priori weight of an observation i using gravimeter G, is given by

$$p_{i_0} = \frac{1}{\sigma_G^2} \tag{13}$$

with

$$\sigma_G = \mathrm{std}(\mathbf{f}_G) \tag{14}$$

and $\mathbf{f}_G$ is the vector that contains the residuals of all the gravity lines measured with gravimeter G. The weight matrix $\mathbf{P}$ is diagonal (since we consider no covariance between observations, as mentioned before), and it contains the observation's weights computed using Eq. (13). In contrast, SCEs are weighted according to the uncertainties of the AG measurements. The weight of the jth SCE is

$$p_{j_0} = \frac{1}{\sigma_j^2} \tag{15}$$

where σ_j is the uncertainty of the AG measurement introduced in the jth SCE. Since $\sigma_G \gg \sigma_j$, SCEs have a significantly larger weight than the observation equations, yet they are not entirely fixed. The weight matrix $\mathbf{P}_{\mathrm{K}}$ contains the SCEs weights computed with Eq. (15) in its diagonal and zeros elsewhere.

Finally, we obtain the weighted least squares gravity solution using Eq. (12). The residuals are obtained from

$$\mathbf{v} = \mathbf{d} - \mathbf{B}\overline{\mathbf{x}} \tag{16}$$

$$\mathbf{v}_{\mathrm{K}} = \mathbf{d}_{\mathrm{K}} - \mathbf{K}\overline{\mathbf{x}} \tag{17}$$

where $\mathbf{v}$ and $\mathbf{v}_{\mathrm{K}}$ are the residual vectors corresponding to the observations and the constraints, respectively. The a posteriori covariance matrix that contains the variances of the adjusted gravity values is calculated in the usual way:

$$\boldsymbol{\Sigma}_{\mathrm{x}} = \widehat{\sigma}_0^2(\mathbf{N} + \mathbf{N}_{\mathrm{K}})^{-1} \tag{18}$$

where $\widehat{\sigma}_0^2$ is the a posteriori variance of unit weight, computed as

$$\widehat{\sigma}_0^2 = \frac{\mathbf{v}^{\mathrm{T}}\mathbf{P}\mathbf{v} + \mathbf{v}_{\mathrm{K}}^{\mathrm{T}}\mathbf{P}_{\mathrm{K}}\mathbf{v}_{\mathrm{K}}}{a - n + h} \tag{19}$$

with a being the number of RG observations, n the number of unknowns (gravity stations), and h the number of SCEs.

6.4 Reweighting procedure

We perform an initial adjustment with the a priori weights and obtain a set of residuals using Eq. (16). To remove the effects of any outliers, we downweight observations with residuals greater than 2.5 sigma (confidence interval of ~ 99%). To do this, we first normalize Eq. (16) using the standard deviation of the residuals:

$$S_i = \mathrm{abs}(v_i/\mathrm{std}(\mathbf{v})) \tag{20}$$

where v_i is the ith residual and S_i is its normalized (or scaled) version. In essence, S_i quantifies the number of standard deviations, whereby each residual deviates from the model. Observations where $S_i \geq 2.5$ are considered outliers and therefore downweighted according to an exponential weighting function

$$p_i = \frac{10^{(2.5-S_i)}}{\sigma_G^2}. \tag{21}$$

The weights of all other observations with $S_i < 2.5$ are computed following Eq. (13).

The newly formed weight matrix $\mathbf{P}$ is used to perform the adjustment again and compute an updated solution that is less affected by outliers. The updated $\widehat{\sigma}_0^2$ value (calculated using Eq. (19)) should now be tested against the a priori variance of unit weight (set equal to one) through a goodness-of-fit test (Ghilani and Wolf 2006). If the test passes, the algorithm stops, and the network gravity solution is final. However, if the test fails, another reweighting iteration occurs, updating

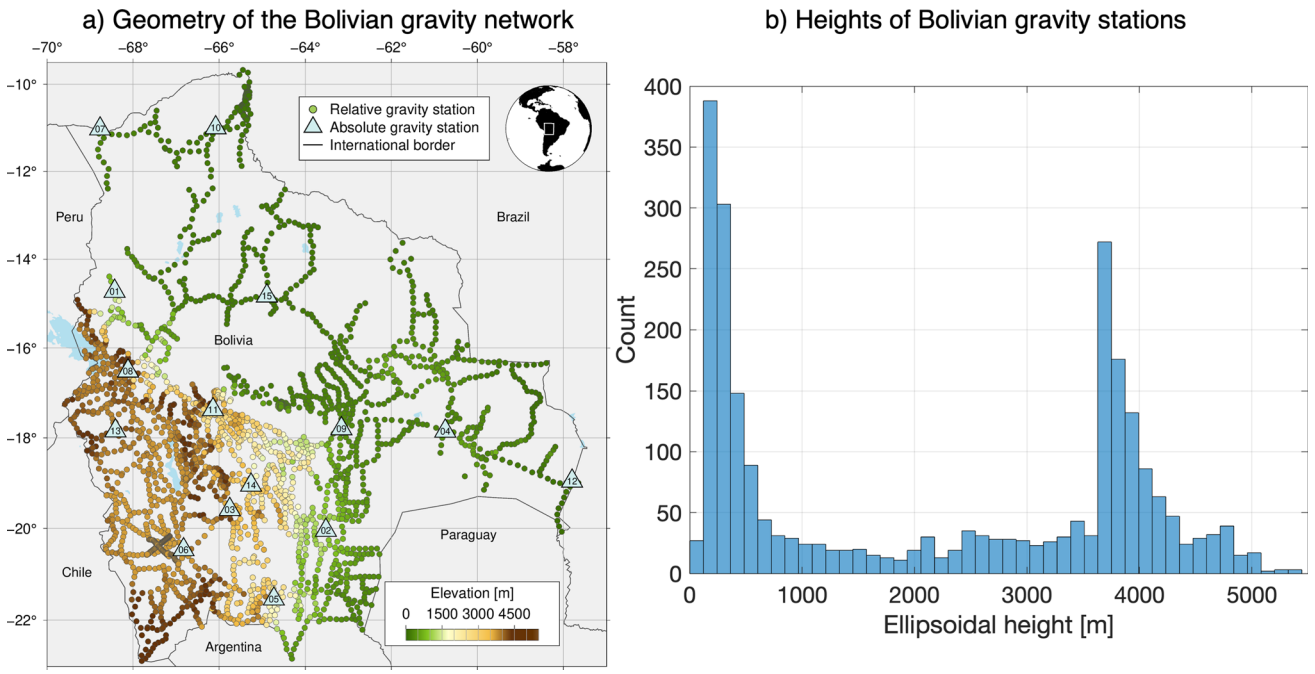

Fig. 6 Bolivian gravity network. **a** Network map totaling 2548 RG stations, and 15 AG stations identified with numbers 01–15. Colors represent the ellipsoidal heights of the gravity stations. **b** Histogram of gravity station's ellipsoidal heights. The minimum and maximum heights are 97.89 m and 5424.24 m, respectively

the weight matrix $\mathbf{P}$ with the new estimate for $\widehat{\sigma}_0^2$. In the $(l+1)^{\text{th}}$ iteration, the updated weight matrix $\mathbf{P}$ is

$$\mathbf{P}|_{l+1} = \frac{1}{\widehat{\sigma}_0^2|_l} \cdot \mathbf{P}|_l. \tag{22}$$

Any newly detected outliers are also downweighted during this step. Unless a severe problem with the input data exists, this process should converge in a small number of iterations (usually two or three). Once the goodness-of-fit test is passed, the final AG values are reported for all stations. Their respective formal errors can be directly computed as the square root of the diagonal elements of $\mathbf{\Sigma}_x$ (obtained using Eq. (18)).

The network adjustment is repeated whenever new gravity lines are measured or existing ones are remeasured. This enhances the overall robustness of the network, as the entire gravity solution is updated using a larger dataset. However, as the network becomes more consolidated, gravity estimates at already existing stations should not change significantly between consecutive network adjustments.

7 The Bolivian gravity network: a case study

The Bolivian gravity network was successfully established, reduced, and adjusted, implementing the OSU field protocol and adjustment methodology. It is composed of 2548 RG stations and 15 AG stations, spanning a wide range of elevations, including (from East to West) the lowlands, the zone of deep valleys, the high Eastern Cordillera, the Altiplano and the Western Cordillera (Fig. 6).

The AG network was measured over the course of one month using a Micro-g LaCoste A10 absolute gravimeter in a collaborative effort between Instituto Geográfico Militar de Bolivia (IGMB), OSU, and the Technical University of Denmark (DTU). Three of the AG sites are reoccupation of previously established stations originally measured with an FG5 absolute meter in the mid 1990's, while the remaining twelve are newly established sites. The typical procedure involved taking two measurements with different instrument setups. Each setup consisted of six sets of a minimum of 100 drops. The AG values were determined with an average precision of $\pm$ 11 μGal.

Surveying the entire RG network presented numerous challenges due to the suboptimal state of the transportation

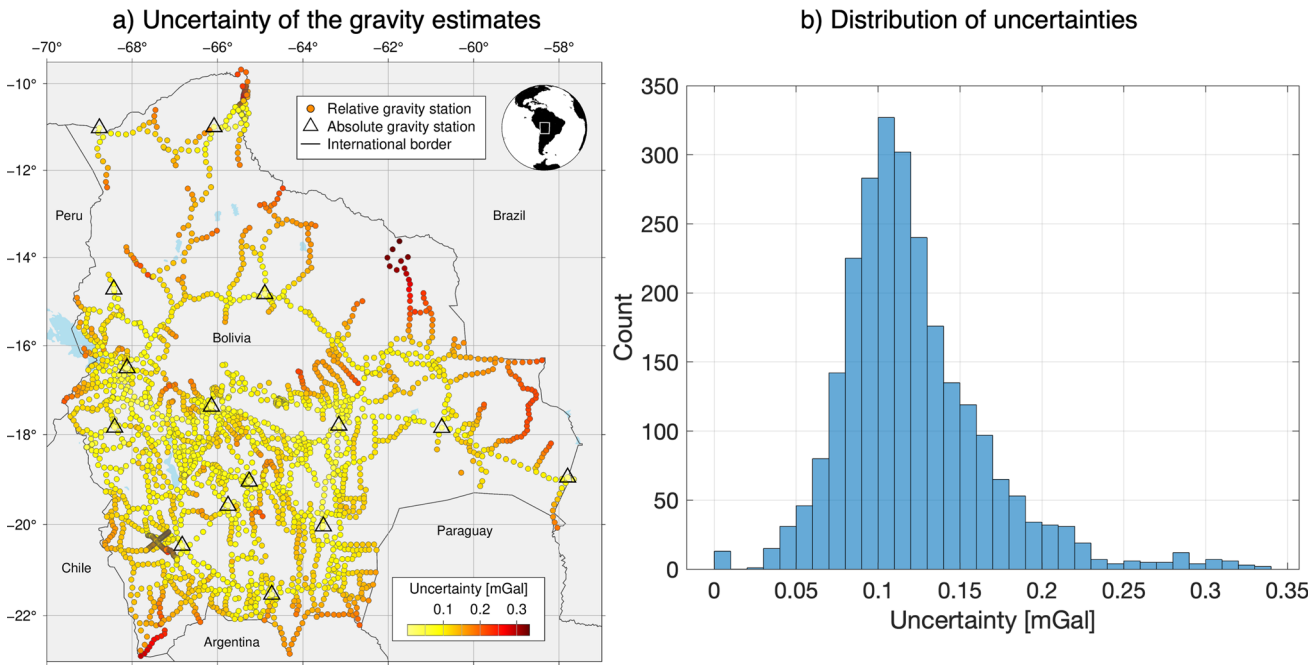

Fig. 7 Uncertainty of the gravity estimates in the Bolivian gravity network. **a** Map of the spatial distribution of uncertainties and location of absolute gravity stations. **b** Histogram of uncertainties of the estimated gravity values (total count: 2548)

infrastructure across the Bolivian territory, which occasionally poses real safety hazards. Roads are often slow and winding, sometimes clinging to near vertical faces of rock, and quite often lacking in regular maintenance. In several regions, it is necessary to ford rivers without bridges and traverse lowland areas with dense vegetation. The additional redundancy in observations that the OSU field protocol yields has proven to be particularly advantageous to building this network, as revisiting such extreme environments to remeasure or rectify subpar measurements is not always practical in Bolivia. We surveyed a total of 513 gravity lines over 12 years. Each line was measured with at least two and, on average, three LaCoste & Romberg Model G gravimeters (although it is worth mentioning that the methodology has also been tested in other locations employing a combination of LaCoste & Romberg, Scintrex CG-5, and Scintrex CG-6 devices). Most gravity lines are composed of 4–8 stations 10–20 km apart. Despite the harsh environmental conditions, 93% of the gravity lines were closed within 36 h and 71% within 24 h.

The acceleration due to gravity has been determined at each station with a typical level of uncertainty (1 sigma) ranging from 0.10 to 0.15 mGal (Fig. 7). The magnitude of the uncertainty at each gravity station mostly depends on three factors: the station's level of connectivity within the network, the number of gravimeters used to make the RG measurements, and the distance to the nearest AG station. The stations showing the most significant uncertainty values (~ 0.33 mGal) are at the end of hanging lines near the edges of the network (Fig. 7a).

Figure 8a shows all the residuals produced by the network adjustment. The symmetry of the distribution suggests the absence of significant systematic errors or evident biases in the model predictions. Figure 8b presents the adjustment residuals excluding outliers. The similarity between the interquartile range (IQR) and the RMS of the residuals in Fig. 8b showcases the robustness of the outlier detection algorithm. Moreover, although the residuals are not normally distributed, the goodness-of-fit filter only flags ~ 2% of the observations as outliers, which matches the confidence interval used during the reweighting scheme (2.5 sigma). Achieving this level of precision in such harsh measurement conditions can be attributed to the OSU field protocol, which ensures the high quality of the data that enters the network adjustment.

7.1 Validation

We assessed the robustness and reliability of our methodology through a leave-one-out cross-validation (LOOCV) using the AG stations of the Bolivian gravity network. This procedure involves removing one AG station constraint at a time, adjusting the gravity network keeping the remaining AG constraints, and then comparing the gravity estimate for the removed constraint against its known 'true' value. The

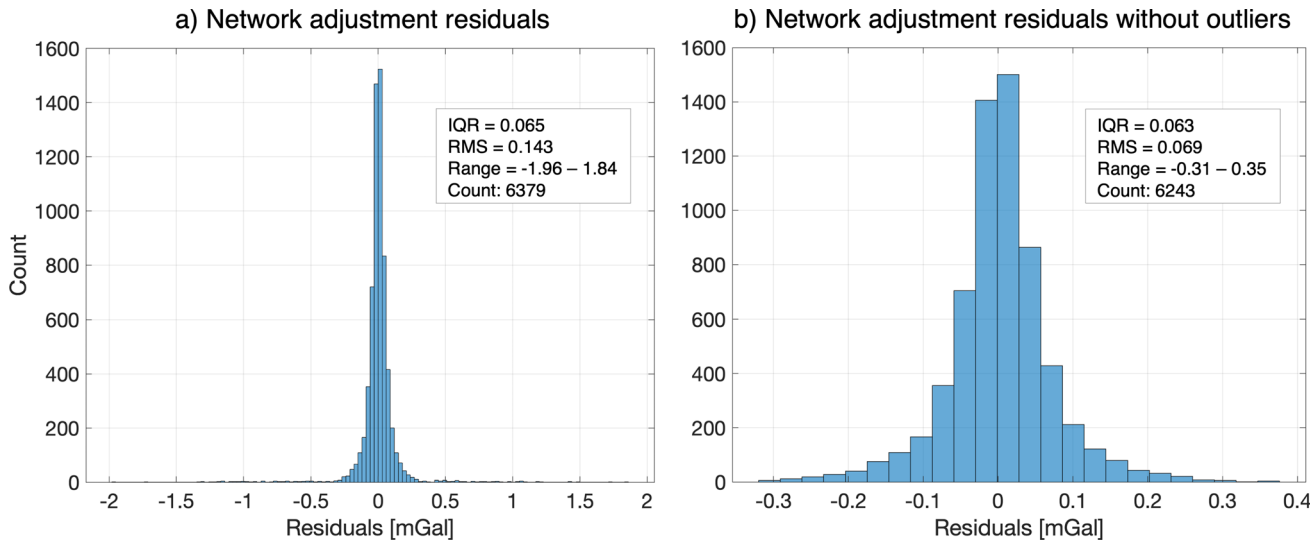

Fig. 8 Histogram of residuals of the Bolivian gravity network adjustment. Residuals are computed as the difference between the adjusted and the observed Δg values. **a** Residuals, including outliers. **b** Residuals, after outliers have been rejected

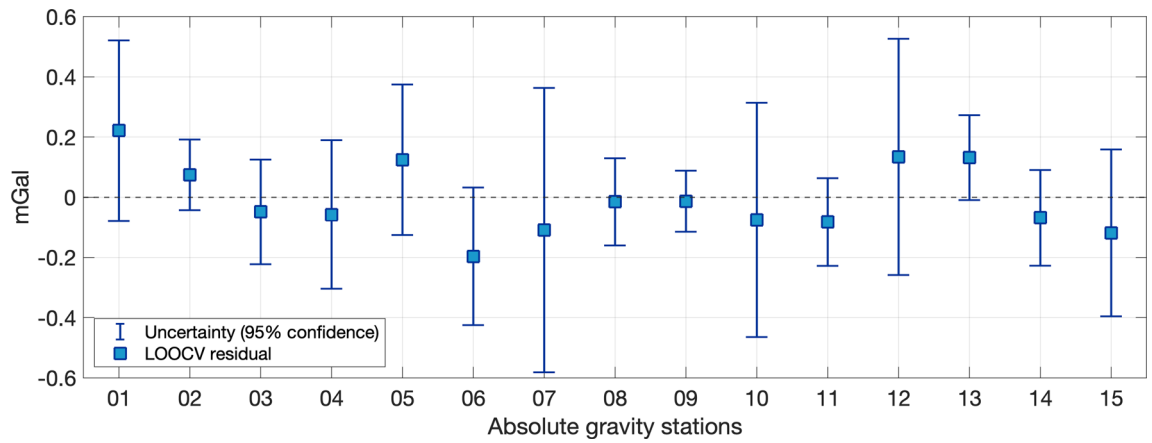

Fig. 9 Results from the LOOCV test. Each residual is the difference between the relative gravity estimate at the station and its absolute gravity value. The gravity estimate is obtained by adjusting the network after removing the constraint at that specific station, while keeping the remaining AG constraints. Error bars show the uncertainties, computed as the square root of the sum of the squared AG uncertainty and the squared estimated relative uncertainty, reported to a 95% confidence interval. The dashed line indicates the zero-residual level. The location of each AG station is shown in Fig. 6

process is repeated for each constraint in the network, generating a set of residuals that serves as an unbiased measure of the methodology's accuracy. Since the Bolivian network has 15 AG stations, each validation adjustment is conducted applying 14 SCEs. Figure 9 shows the residuals obtained for each test and their reported uncertainty (95% confidence interval).

The validation shows that the zero-residual level falls within the 95% confidence interval at every AG station, and all the residuals are below the network's maximum reported uncertainty (Fig. 7b). We found a residual mean of -0.006 mGal, well below the noise level of ~ 0.06 mGal, showing that the network adjustment does not introduce significant biases. Lastly, the standard deviation of the residuals is 0.117 mGal, in agreement with the expected uncertainty reported for the network adjustment (Fig. 7).

8 Conclusions

We presented a comprehensive methodology to plan, survey, process, and adjust large relative surface gravity networks. Our approach relies on a 'defensive' field protocol designed to achieve very high degrees of observational redundancy, and a two-step least squares adjustment scheme focused on fully exploiting this redundancy. Our methodology guarantees reliable adjusted gravity estimates unaffected by

observation outliers, and well-constrained standard error estimates calculated based on physically meaningful residuals.

The presented method was implemented in a MATLAB package, GRAVITAS, featuring a graphical user interface (GUI) conveniently separated using different modules. This software enables users to load gravity lines surveyed using multiple gravimeters, apply calibration and gravity tide corrections, perform visual and statistical checks, and adjust each line individually before combining them in a robust network adjustment. Although the software was designed to leverage the redundancy in observations produced by the OSU protocol, it can also handle input data produced by a standard occupation procedure (Fig. 3a). We also developed an Android application to collect field data using mobile devices. The app allows loading georeferenced (and time tagged) field gravity data and pictures of each measurement, and also performs real-time line closure checks. The use of the app is not a requirement for using our measurement protocol, but it has proven to be a useful tool to reduce the occurrence of reading and time recording errors and expedite the data collection process.

Lastly, we presented the case study of the Bolivian gravity network. Despite being surveyed under adverse environmental and logistical conditions and spanning a wide range of elevations (Fig. 6), the acceleration due to gravity was determined at 2548 stations with a typical level of uncertainty (1 sigma) of 0.10–0.15 mGal. We validated these results using a LOOCV test applied to all the AG stations across the network, and verified that our methodology can estimate AG with an error that is within the predicted uncertainty.

It is worth noting that the Central Andes, characterized by diverse terrain and geography, provide an interesting test laboratory for gravity modeling. Here, observing a gravimetric network requires different and more defensive methodologies than would be utilized in many other parts of the world. Previous works have emphasized the need to fill gravity data gaps in remote areas, such as mountain tops and jungles, as a critical step toward the realization of the IHRS (e.g., Sánchez et al. 2021). In this context, our methodology becomes a valuable tool for achieving this goal, given the efficacy demonstrated under the very harsh field conditions prevailing in much of Bolivia and its potential utility in similarly challenging settings.

Supplementary Information The online version contains supplementary material available at https://doi.org/10.1007/s00190-024-01891-w.

Acknowledgements FSS, MGB, and DDG would like to thank Ezequiel Antokoletz for providing additional information regarding the gravity measurement protocol implemented by Instituto Geográfico Nacional de Argentina (IGN) and for discussions about differing models of gravity and earth tides. We thank Andres H. Pityla for developing the Android interface of the app Log4G to record gravity observations. We also thank the responsible editor and two anonymous reviewers for their constructive criticism and suggestions to improve the manuscript.

Author contributions KA, MGB, and AE developed the field measurement protocol. KA, MGB, DDG, and FSS developed the adjustment methodology. KA and DDG implemented the adjustment method into a MATLAB package (GRAVITAS). DDG and Andrés H. Pityla conceptualized the Android app Log4G for field data collection. KA, MGB, JH, FSS, EK, PM, LCC, AB, JCC, RTS, and HGT made the gravity measurements in Bolivia. AE, DJC, KA, JH, RTS, and EK did the GNSS positioning of the gravity stations. FSS, KA, MGB, DDG, and DJC wrote the manuscript. FSS created Figs. 1, 2, 3, 4, 5, 6, 7, 8, and 9, Table 1, and Figs. S1 and S2. All authors approved the manuscript.

Funding This work was financially supported by the US government. Sobrero also acknowledges support from the Division of Geodetic Science, School of Earth Sciences, Ohio State University, and the Friends of Orton Hall Fund.

Data availability The Bolivian gravity network is presented as a case study solely for the purpose of demonstrating the performance of the OSU field protocol and adjustment methodology. Scientists and agencies seeking access to the gravity data should write to Prof. M. Bevis at Ohio State University. Figures were generated with Generic Mapping Tools (Wessel et al. 2019) and Adobe Illustrator.

Code availability The MATLAB package GRAVITAS to run the two-step adjustment is openly available through https://github.com/demiangomez/GRAVITAS. The Android app Log4G to record gravity observations in the field is available through https://github.com/lateral-search/Log4G.

Declarations

Conflict of interest The authors declare that they have no conflict of interest.

References

Baarda W (1967) Statistical concepts in geodesy. Waltman, Delft

Bonvalot S, Diament M, Gabalda G (1998) Continuous gravity recording with Scintrex CG-3M meters: a promising tool for monitoring active zones. Geophys J Int 135:470–494. https://doi.org/10.1046/j.1365-246X.1998.00653.x

Büllesfeld F-J (1985) Ein Beitrag zur harmonischen Darstellung des gezeitenerzeugenden Potentials. Deutsche Geodaetische Kommission Bayer Akad Wiss 314:

Cartwright DE, Edden AC (1973) Corrected tables of tidal harmonics. Geophys J Int 33:253–264. https://doi.org/10.1111/j.1365-246X.1973.tb03420.x

Cartwright DE, Tayler RJ (1971) New computations of the tide-generating potential. Geophys J Int 23:45–73. https://doi.org/10.1111/j.1365-246X.1971.tb01803.x

Dias FJSS, Escobar IP (2001) A model for adjustment of differential gravity measurements with simultaneous gravimeter calibration. J Geodesy 75:151–156. https://doi.org/10.1007/s001900100168

Diouf D, Ndiaye M, Morel L (2023) Precise point positioning and differential solutions by online GNSS calculation tools and RTKLIB: a comparative study. Int J Geosci 14:226–237. https://doi.org/10.4236/ijg.2023.142011

Doodson AT (1921) The harmonic development of the tide-generating potential. Proc Royal Soc London Ser Contain Papers Math Phys Charact 100:305–329. https://doi.org/10.1098/rspa.1921.0088

Eckl MC, Snay RA, Soler T et al (2001) Accuracy of GPS-derived relative positions as a function of interstation distance and observing-session duration. J Geodesy 75:633–640. https://doi.org/10.1007/s001900100204

FGCC (1984) Standards and specifications for geodetic control networks. Federal Geodetic Control Committee, Rockville

Fores B, Champollion C, Moigne NL, Chery J (2017) Impact of ambient temperature on spring-based relative gravimeter measurements. J Geod 91:269–277. https://doi.org/10.1007/s00190-016-0961-2

Ghilani CD, Wolf PR (2006) Adjustment computations: spatial data analysis. Wiley, Hoboken

Goodkind JM (1986) Continuous measurement of nontidal variations of gravity. J Geophys Res 91:9125–9134. https://doi.org/10.1029/JB091iB09p09125

Grinter T, Janssen V (2012) Post-processed precise point positioning: a viable alternative? In: Proceedings APAS2012. Wollongong, Australia

Hamilton AC, Brulé BG (1967) Vibration-induced drift in LaCoste and Romberg geodetic gravimeters. J Geophys Res 1896–1977(72):2187–2197. https://doi.org/10.1029/JZ072i008p02187

Hinze WJ, Von Frese R, Saad AH (2013) Gravity and magnetic exploration: principles, practices, and applications. Cambridge University Press, New York

Hwang C, Wang C-G, Lee L-H (2002) Adjustment of relative gravity measurements using weighted and datum-free constraints. Comput Geosci 28:1005–1015. https://doi.org/10.1016/S0098-3004(02)00005-5

IBGE (2017) Especificações e Normas para Levantamentos Geodésicos Associados ao Sistema Geodésico Brasileiro. In: Instituto Brasileiro de Geografia e Estatística, Brasil. https://geoftp.ibge.gov.br/metodos_e_outros_documentos_de_referencia/normas/normas_levantamentos_geodesicos.pdf. Accessed 17 Apr 2024

IGN (2014) Instrucciones Técnicas de Campaña y Gabinete. Instituto Geografico Nacional, Argentina, Buenos Aires, Argentina

INEGI (2015) Guía Metodológica de la Red Geodésica Gravimétrica. In: Instituto Nacional de Estadistica y Geografia, Mexico. https://www.inegi.org.mx/app/biblioteca/ficha.html?upc=702825078799. Accessed 17 Apr 2024

Kanngieser E (1983) Genauigkeitssteigerungen in der Relativgravimetrie. Zeitschrift Fuer Vermessungswesen 108:180–189

Klees R, Reudink RHC, Flikweert PLM (2019) Tilt susceptibility of the Scintrex CG-5 autograv gravity meter revisited. In: Vergos GS, Pail R, Barzaghi R (eds) International symposium on gravity, geoid and height systems 2016. Springer, Cham, pp 119–123

Koch KR (2013) Parameter estimation and hypothesis testing in linear models. Springer, Berlin

LaCoste & Romberg (2004) Instruction Manual—Model G & D Gravity Meters. Austin, TX, USA

Lambert A, Liard J, Dragert H (1979) Canadian precise gravity networks for crustal movement studies: an instrument evaluation. Tectonophysics 52:87–96. https://doi.org/10.1016/0040-1951(79)90209-9

Longman IM (1959) Formulas for computing the tidal accelerations due to the moon and the sun. J Geophys Res 1896–1977(64):2351–2355. https://doi.org/10.1029/JZ064i012p02351

Merriam JB (1992) Atmospheric pressure and gravity. Geophys J Int 109:488–500. https://doi.org/10.1111/j.1365-246X.1992.tb00112.x

Murray AS, Tracey RM (2001) Best Practice in Gravity Surveying. Geoscience Australia, Canberra

Niebauer T (2015) gravimetric methods–absolute and relative gravity meter: instruments concepts and implementation. Treatise on Geophysics. Elsevier, Amsterdam, pp 37–57

Poutanen M, Rózsa S (2020) The geodesist's handbook 2020. J Geod 94:109. https://doi.org/10.1007/s00190-020-01434-z

Reudink R, Klees R, Francis O et al (2014) High tilt susceptibility of the Scintrex CG-5 relative gravimeters. J Geod 88:617–622. https://doi.org/10.1007/s00190-014-0705-0

Rymer H (1989) A contribution to precision microgravity data analysis using lacoste and romberg gravity meters. Geophys J Int 97:311–322. https://doi.org/10.1111/j.1365-246X.1989.tb00503.x

Scintrex Limited (2012) Scintrex Operation Manual, Model CG-5. https://scintrexltd.com/support/product-manuals/. Accessed 17 Apr 2024

Sánchez L, Ågren J, Huang J et al (2021) Strategy for the realisation of the international height reference system (IHRS). J Geod 95:33. https://doi.org/10.1007/s00190-021-01481-0

Shouny AE, Miky Y (2019) Accuracy assessment of relative and precise point positioning online GPS processing services. J Appl Geodesy. https://doi.org/10.1515/jag-2018-0046

Soler T, Michalak P, Weston ND et al (2006) Accuracy of OPUS solutions for 1- to 4-h observing sessions. GPS Solut 10:45–55. https://doi.org/10.1007/s10291-005-0007-3

Tamura Y (1987) A harmonic development of the tide-generating potential. Bull D'information Marees Terrestres 99:6813–6855

Torge W (1989) Gravimetry. Walter de Gruyter, Berlin

Van Camp M, de Viron O, Watlet A et al (2017) Geophysics from terrestrial time-variable gravity measurements. Rev Geophys 55:938–992. https://doi.org/10.1002/2017RG000566

Van Mierlo J (1980) Free network adjustment and S–Transformations. Deutsche Geodätische Kommission, Reihe B, Heft Nr. 252, München:

Wessel P, Luis JF, Uieda L et al (2019) The generic mapping tools version 6. Geochem Geophys Geosyst 20:5556–5564. https://doi.org/10.1029/2019GC008515